M2 - IPParis - Advanced Experimental Methods in Fluid Mechanics
Acquisition - Signal processing

Romain Monchaux, ENSTA-Paris - Institut Polytechnique de Paris
(monchaux@ensta.fr)

1 Gaussian white noise

1.1 Average, standard deviation and probability density function

Question 1 : raw signals visualised at different scales are shown in figure 1. The signal is highly fluctuating. It seems to be statistically stationary with a zero average and a standard deviation close to 1.

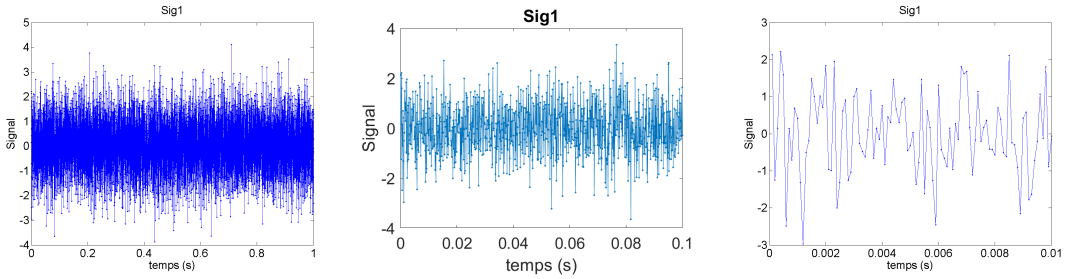

FIGURE 1 – Signal 1 visualised at different time scales.

Question 2 : The required plot is given in figure 2. We clearly see that the average and the standard deviation are well estimated when the number of points used to do so is rather important (of the order of $10^4 0 at least$). We do not exactly recover what has been said during the lecture since the presented results where obtained from a large ensemble of realisations of the same Gaussian white noise, but nevertheless, the global trend is the same, a convergence toward the two first moments as $1/\sqrt{(N)}$.

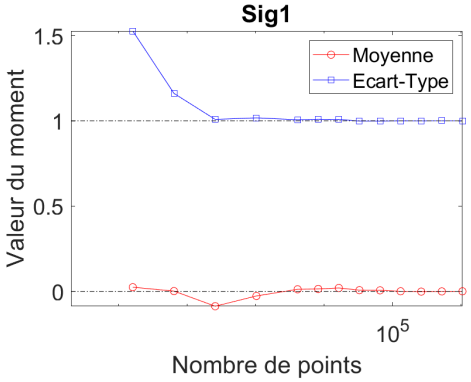

FIGURE 2 – Evolutions of the estimated average and standard deviation with the length of the considered signals.

Question 3 : We set the number of points NbPt at 2^{20} and the number of bins at 100. We plot the three different representation of the PDF in figure 3. Each representation allows to check the PDF estimation quality.

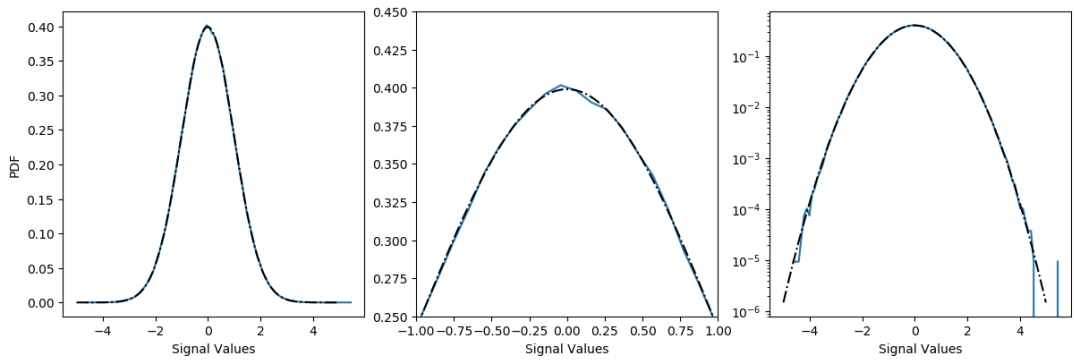

FIGURE 3 – Different representation of the PDF. From left to right : in linear scale, a zoom around the maximum in linear scale, in semi-logarithmic scale.

Question 4 : We choose different number of points NbPt, here 2^{10}, 2^{12}, 2^{16}, 2^{18} et 2^{20}. The "optimal" values for the number of bins used in the PDF estimation is chosen so that the maximum of the PDF is not too noisy in linear representation while the tails are found as long as possible with a minimal noise level in logarithmic scale. Figure 4 gathers the results. The number of bins required to best capture the PDF increases with the number of data points. Figure 5 presents the "optimal" values found. We see that they evolve as the signal length to the power 1/3.

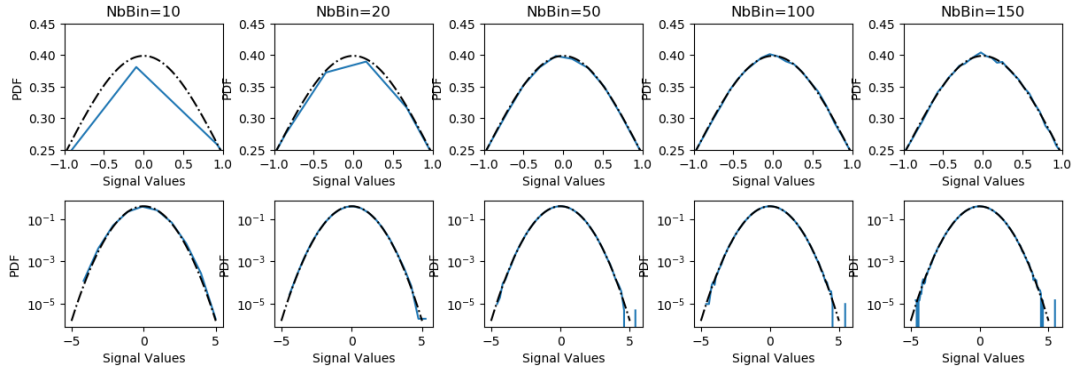

FIGURE 4 – PDF evolution with the number of bins used to compute them for a signal of length 2^{16}.

1.2 Spectrum and autocorrelation

Question 1 : Figure 6 presents the Gaussian white noise spectra obtained for four different window lengths. The shorter the window, the less noisy is the spectrum. This is normal since for a given su=ignal length, if the window size diminish, the function welch will perform more averages between spectra calculated over interval of length Nwindow. As soon as they have converged, the spectra of the gaussian white noise are flat. This is the very nature of this noise to be evenly distributed over all the frequencies. The frequential resolution is the precision we have to distinguish two frequencies. It is directly linked to the sampling frequency and to the number of points used to calculate the FFT. It os given by : $\Delta f = Fs/N_{fft}$.
When we try and estimate the power spectral density of a signal, we have to choose the number of points used to calculate the FFT. This choice results from a balance between the frequential resolution and the

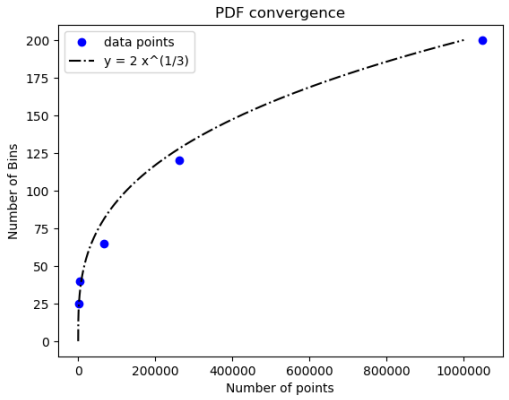

FIGURE 5 – Evolution of the best bins number to estimate the PDF as a function of the signal length.

noise level admitted. A way to increase simultaneously N_{fft} and the level of averaging is to increase the signal duration. Since a signal can not be extended once acquired, one has to think about acquiring long enough signals!

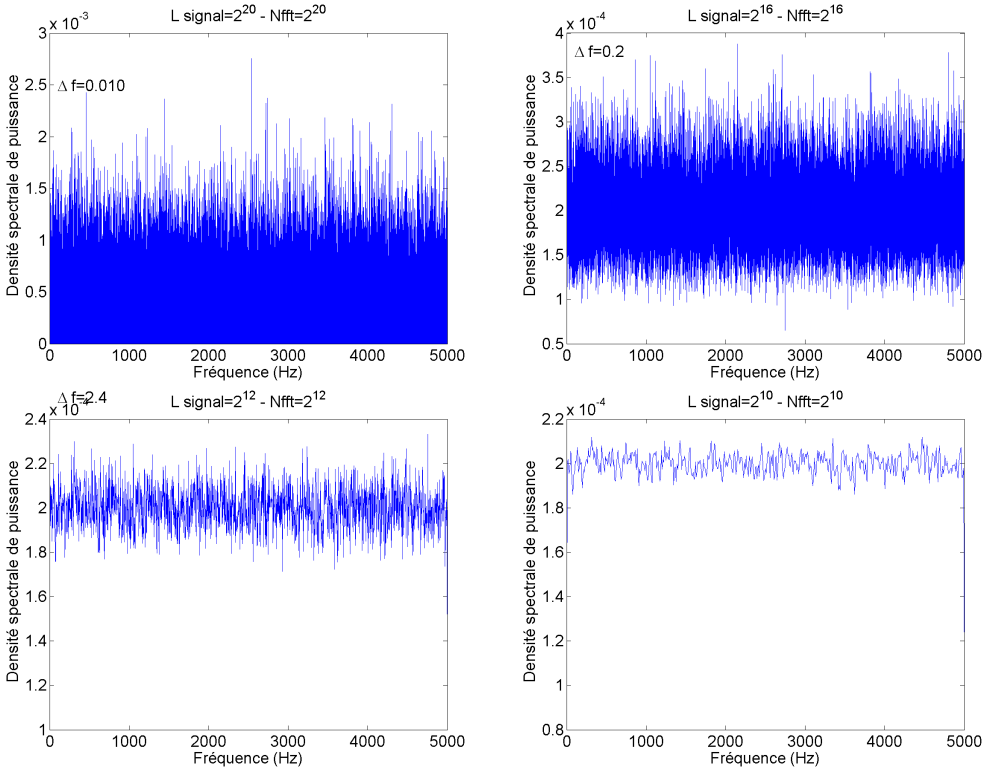

FIGURE 6 – Power spectral density of a Gaussian white noise estimated from different window lengths.

Question 2 : The auto-correlation of the Gaussian white noise is plotted in figure 7. This function is even, we can plot only half of it. We see a peak to 1 at 0 which is systematic for the normalised auto-correlation. Otherwise it is very close to 0 everywhere. this is due to the fact that two successive samples of the Gaussian white noise are uncorrelated.

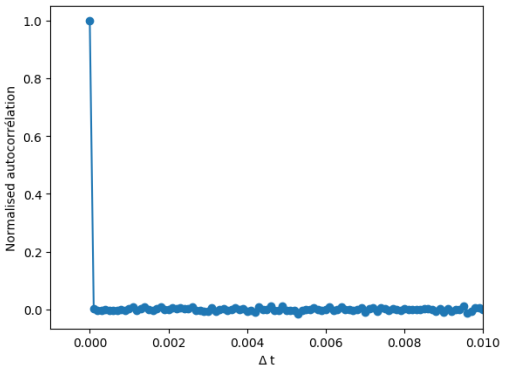

FIGURE 7 – Auto-correlation of the Gaussian white noise.

2 Study of three synthetic signals

Question 1 : The time signals of the three studied signals are shown in figure 8 for three different time zoom. They all are very fluctuating, they all ressemble the Gaussian white noise studied earlier, they may thus all contain energy on a wide range of scales. We can notice that signal 2 has to be looked at on a time scale 10 times longer than the others to ressemble them. From what we have just said, their spectra should cover all frequencies, the first signal on a more restricted range obviously. They all have the same mean (0) and standard deviation (1). Signal 2 seems more correlated than the others.

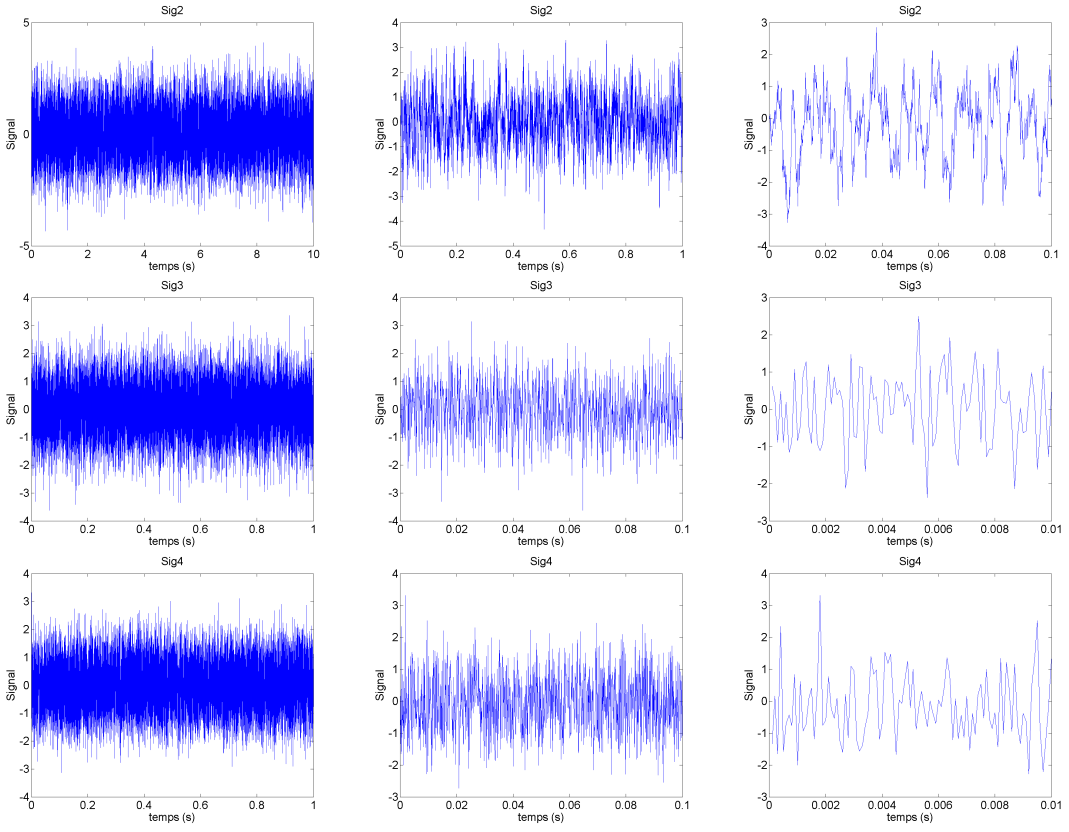

FIGURE 8 – Time trace of the three studied signals.

Question 2 : The three requested spectra are plotted in figure 9.

— Signal 2 has a flat spectrum at low frequencies, with a rapid drop towards high frequencies with a power law slope of about −1.7.
— Signal 3 has a flat white Gaussian noise spectrum, with two well defined peaks at 1000 Hz and 2500 Hz. It could therefore correspond to the sum or product of two noisy sine waves by a white Gaussian noise.
— Signal 4 has a flat white Gaussian noise spectrum.

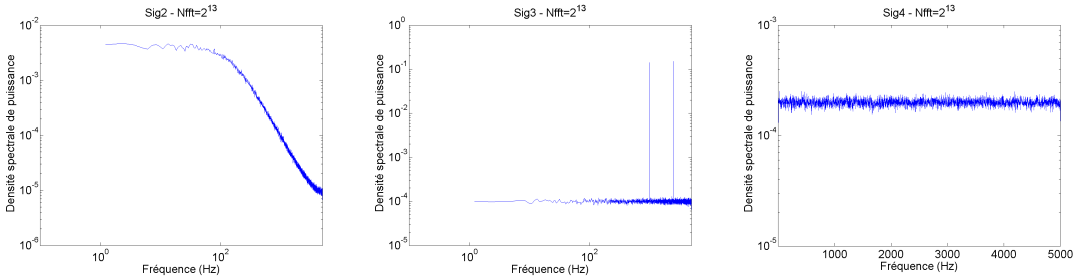

FIGURE 9 – Power spectral density of the three studied signals.

Question 3 : The probability densities obtained from 2^{12} points for each of the three signals are shown in Figure 3**??**. All three probability densities are reasonably Gaussian, although the probability density for Signal 4 seems to be a bit flattened around 0.

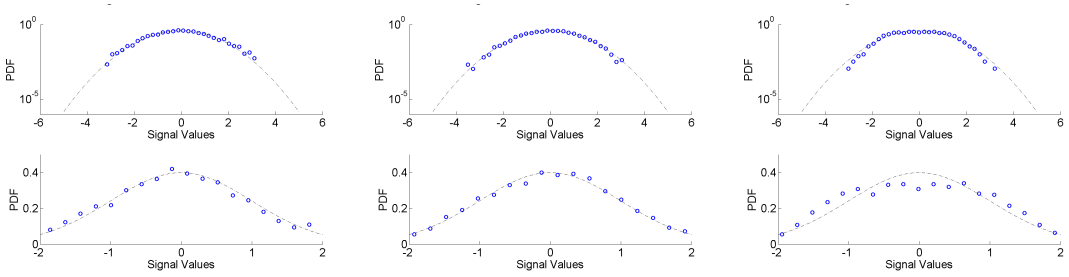

FIGURE 10 – Probability density of the three studied signals obtained from 2^{12} points.

Question 4 : By working with the full signals, see figure 11, we find the two Gaussian for Signal 2 and Signal 3, on the other hand, we see now that Signal 4 presents a bi-modal distribution with two maxima.

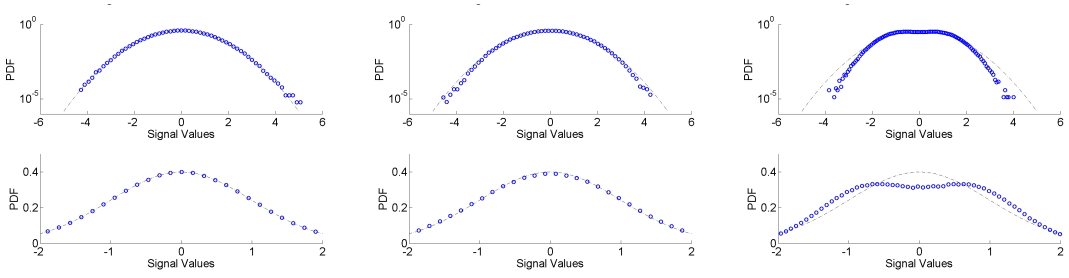

FIGURE 11 – Probability density of the three studied signals obtained from 2^{20} points.

Question 5 : The auto-correlations of the three signals are presented in figure 12. We see that Signal 1 is correlated noise, Signal 2 is periodic, the auto-correlation shows the two frequencies well, the noise has completely disappeared. Signal 3 is delta-correlated in time, like a white Gaussian noise.

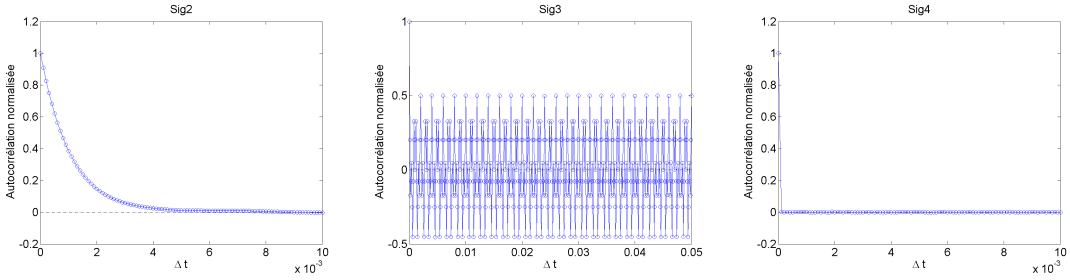

FIGURE 12 – Auto-correlation of the three studied signals obtained from 2^{20} points.

Question 6 et 7 : we have seen that very different signals could have the same statistical moments, even the same PDF or the same spectra or auto-correlation. It is the plot of all these quantities that allowed us to conclude on the nature of the signals studied. In all cases, we needed signals long enough to be able to decide.

3 Real signal anaylisis

3.1 Jet

Question 1 :

1. Different zooms of the turbulent jet velocity signal are shown in Fig. 13.
2. The signal seems stationary, and it also seems to have a rich spectral content. Indeed, at the different zoom levels, there are always fluctuations that seem, at these temporal scales, similar to those observed at higher scales.

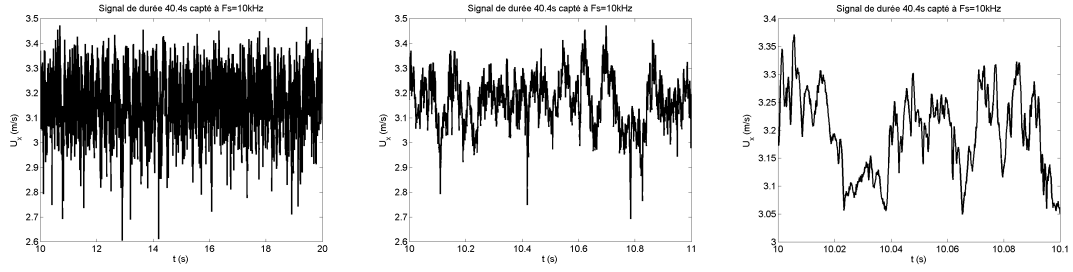

FIGURE 13 – Time signal of the turbulent jet : three zoomed versions.

3. The mean ($\overline{U_x}$) and standard deviation ($u_{x_{rms}}$) of the velocity calculated over time intervals of different lengths are plotted in Fig. 14.
4. The signal seems quite stationary, but is very fluctuating. Indeed, when the averages are realized on short times ($\simeq 0.1s$ and less), the sliding average remains very fluctuating.

Question 2 :

1. the spectrum calculated on the complete signal is presented in figure 15. Its frequency resolution is given by $\Delta f = F_s/N_{FFT}$ and is here 0.0248 Hz.
2. The spectrum is very noisy. This is normal, the Fourier transform contains as much information as the temporal signal, as we did not perform any kind of averaging here, we find a signal that has the same level of noise as the original signal. The bounds of the spectrum are given : at the high frequencies by the Shannon frequency ($F_s/2$) and at the low frequencies by the length of the signal on which the FFT is calculated ($2F_s/N_{FFT}$).

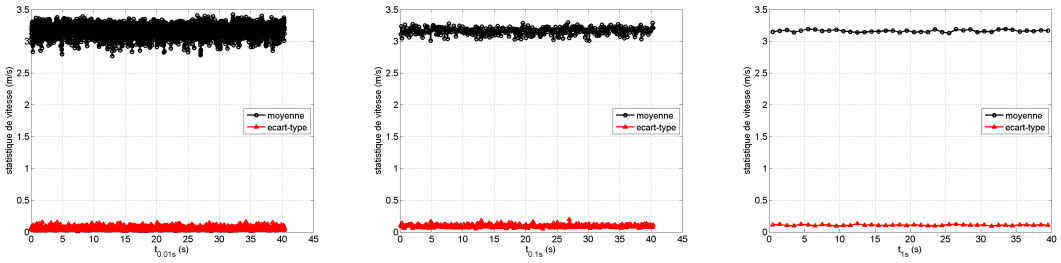

FIGURE 14 – Sliding average and standard deviation of the turbulent jet signal obtained over different averaging horizons of this signal : from left to right (10 ms, 100 ms and 1000 ms).

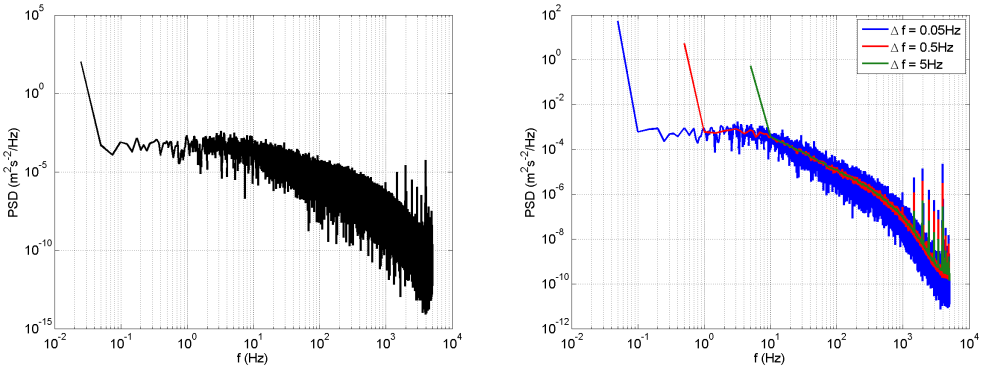

FIGURE 15 – Spectra of the turbulent jet velocity signal. Left : spectrum calculated on the complete signal at a frequency resolution $\Delta f = 0.0248$ Hz. Right : stack of different spectra obtained at different frequency resolutions.

Question 3 :

1. The spectra of the turbulent jet velocity signal obtained at different frequency resolutions ranging from 0.05 Hz to 5 Hz are stacked on the right figure of Fig. 15. The greater the frequency resolution, i.e. the greater the number of averaged spectra, the smoother the signal and the lower the noise level. The upper bound of the spectrum, always given by $F_s/2$, does not vary from one spectrum to another, while the lower bound becomes larger and larger as the averaging level increases. The expected slope for a turbulent velocity spectrum in $f^{-5/3}$ becomes observable only after a certain averaging level. The viscous cut-off is also clearly observed around $f \simeq 800$ Hz.

Question 4 : The auto-correlation and PDF of the jet signal are plotted in Fig. 16. We can see that the jet is correlated over quite long times, which explains that mean and standard deviation converge for quite large numbers of successive samples. This correlation is also seen on the power law spectrum of exponent $-5/3$ as expected from Kolmogorov's work. The probability density is not Gaussian, negative events are more probable than positive ones.

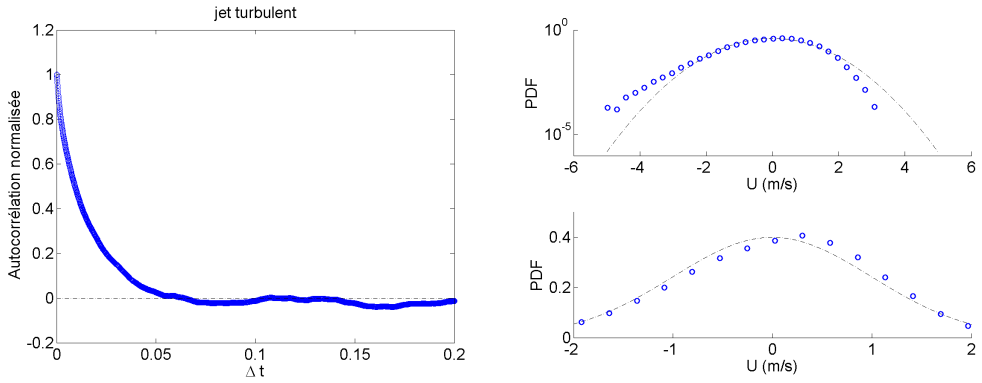

FIGURE 16 – Auto-correlation and probability density of the jet signal.

3.2 Wake

We are now interested in the signal of a turbulent wake captured by a hot wire. The hot wire measures the longitudinal velocity component U_x at the wake axis at about 10 diameters after the cylinder.

Question 1 :

1. Different time zooms of the wake signal are shown in Fig. 17

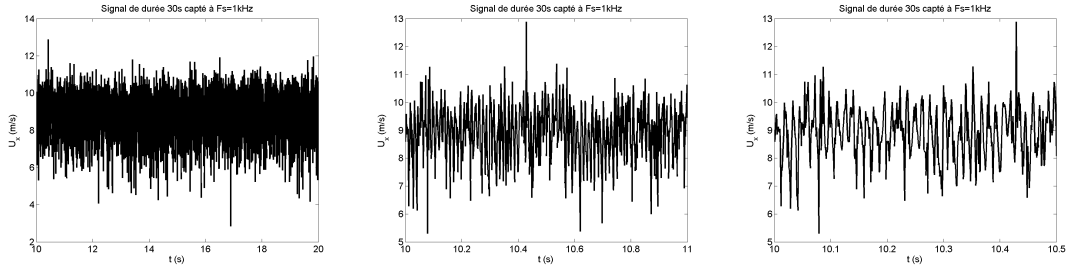

FIGURE 17 – Time signal of the turbulent wake : three zoomed versions.

2. The signal seems stationary. The 500 ms zoomed version seems to have a well defined period around 0.01 s. The signal also shows slower fluctuations that resemble those observed in the turbulent jet.
3. The mean ($\overline{U_x}$) and standard deviation ($u_{x_{rms}}$) of the velocity calculated over time intervals of different lengths are plotted in Fig. 18.

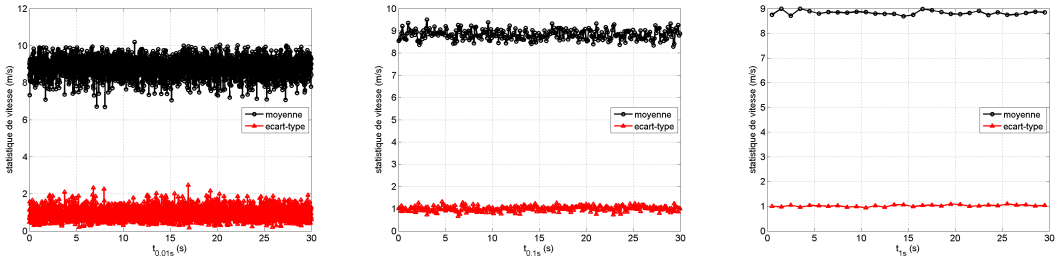

FIGURE 18 – Sliding average and standard deviation of the turbulent wake signal obtained on different averaging horizons of this signal : from left to right (10 ms, 100 ms and 1000 ms).

4. The signal seems quite stationary, but is very fluctuating. Indeed, when the averages are realized on short times ($\simeq 0.1s$ and less), the sliding average remains very fluctuating. This is probably a sign of correlations present at short times.

Question 2 Statistical study.

1. The spectrum of the turbulent wake signal calculated on the complete signal is presented in figure 19. Its bounds are given as before by the Shannon frequency and the FFT horizon. The spectrum is again very noisy for the same reasons as for the jet. It seems to have a peak at a well defined frequency around $F_p \simeq 75$ Hz.
2. The spectra of the turbulent wake velocity signal obtained at different frequency resolutions ranging from 0.05 Hz to 5 Hz are stacked on the right figure of Fig. 19. The greater the frequency resolution, i.e. the greater the number of averaged spectra, the smoother the signal and the lower the noise level. The upper bound of the spectrum, always given by $F_s/2$, does not vary from one spectrum to another, while the lower bound becomes larger and larger as the averaging level increases. On smoother spectra, the frequency around 75 Hz is clearly visible and easily measurable. It corresponds of course to the vortex release of the von Kármán instability which operates here on a turbulent background. The expected slope for a turbulent velocity spectrum in $f^{-5/3}$ becomes observable only after a certain averaging level. The viscous cutoff cannot be observed here, as it must occur at frequencies higher than the sampling frequency.
3. The auto-correlation and probability density of the jet signal are presented in Figure 20. On the auto-correlation, we find the periodicity linked to the Bénard-von Kármán street, the correlation on times is of the order of 0.2 s, longer than in the case of the jet. The PDFs are quite similar to those of the turbulent jet.
4. In conclusion, this signal contains all the characteristics of the turbulent jet to which is added the periodicity related to the unstable mode of Bénard-von Kármán.

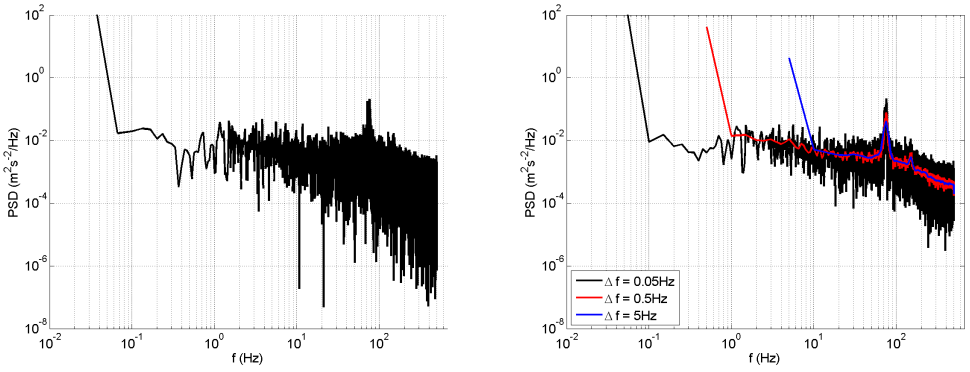

FIGURE 19 – Spectra of the turbulent wake velocity signal. Left : spectrum calculated on the full signal at a frequency resolution $\Delta f = 0.033$ Hz. Right : stack of different spectra obtained at different frequency resolutions.

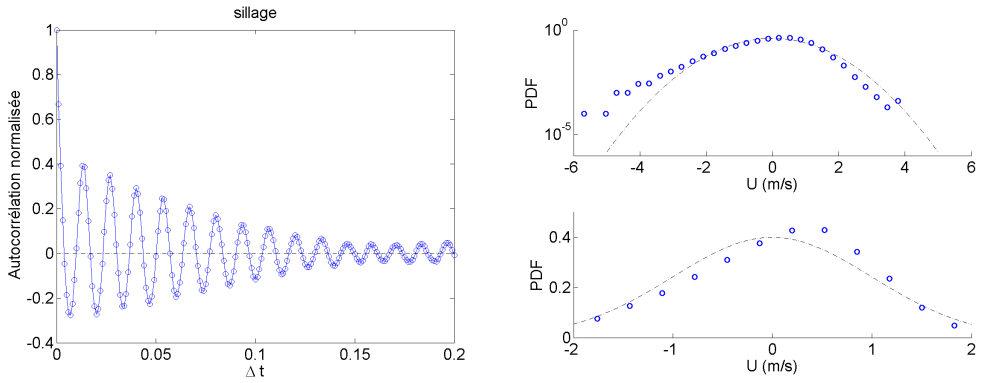

FIGURE 20 – Auto-correlation and probability density of the turbulent wake velocity signal.

3.3 Gong

Question 1 :

1. The forcing signal and the pressure signal are plotted in Figure 21.

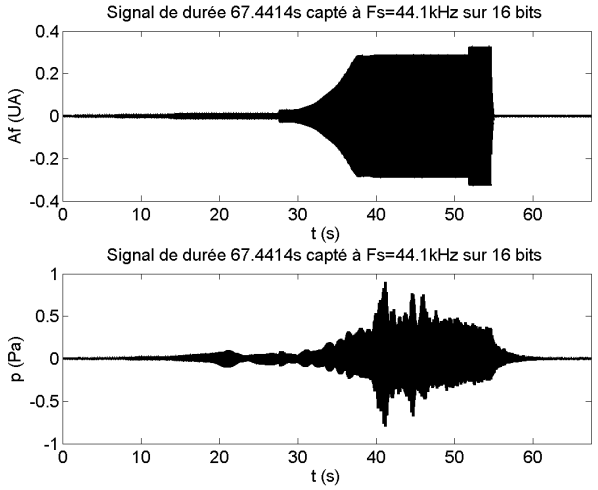

FIGURE 21 – Time signals of the gong : top : forcing, bottom : pressure response. Complete signals.

2. The mean ($overlinep$) and standard deviation (p_{rms}) of pressure and forcing obtained over varying time intervals are plotted in Fig. 22.
3. The signals are clearly not stationary.

Question 2 :

1. The pressure response signal spectrum for the full signal is plotted in linear and logarithmic scale in Fig. 23. In linear scale we see well defined frequency peaks. In logarithmic scale, a slope seems to emerge which could remind the turbulent spectra observed above. As the signal is not stationary, this spectrum calculated on the complete signal must however be commented with circumspection.

Question 3 : The spectrum of the pressure response signal and that of the forcing at a resolution of 5 Hz without overlap are shown in Fig. 24.

1. The time resolution is given by $N_{FFT}/F_s = 1/\Delta f$ and is here 0.2 s.

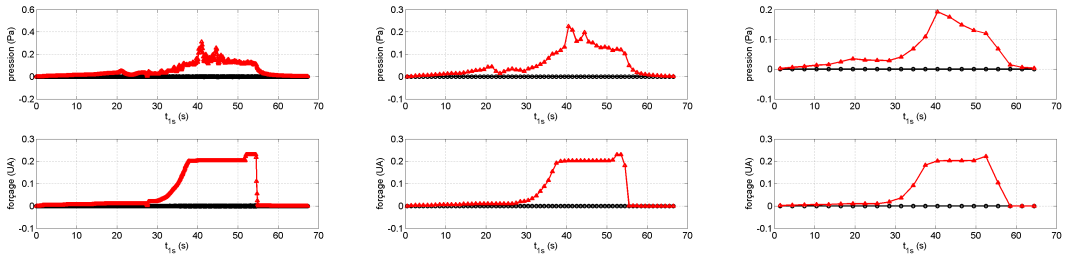

FIGURE 22 – Sliding mean and standard deviation of the gong signal obtained over different averaging horizons of this signal : from left to right (100 ms, 1000 ms and 3000 ms).

.

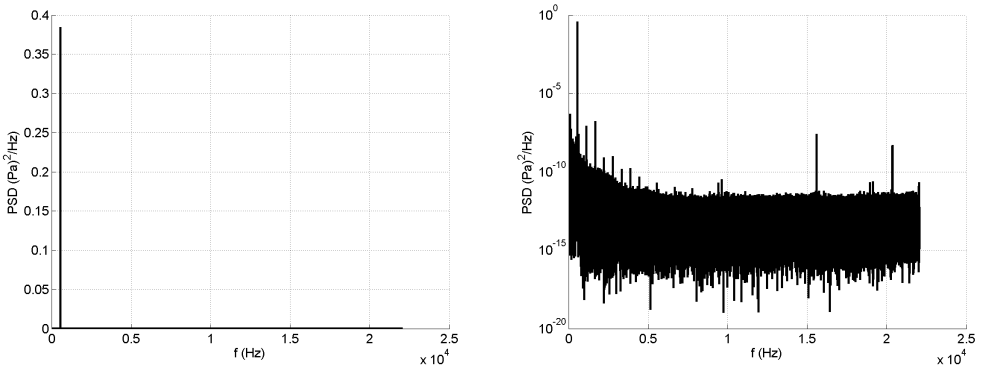

FIGURE 23 – Spectra of the gong pressure response signal computed on the complete signal at a frequency resolution $\Delta f = 0.0148$ Hz. Left : in linear scale. Right : in logarithmic scale.

2. We can increase the temporal resolution, but this will be at the expense of the frequency resolution. Some trial and error show that the choice made here is a good compromise.
3. The pressure response first shows two sharp spectral lines, one centered on the forcing frequency, the other being the first harmonic. The system responds to the excitation in a linear way. From $t \simeq 20$ s, the pressure response shows new frequencies that do not appear to be multiples or submultiples of the forcing frequency. The system begins to respond weakly nonlinearly to excitation. From $t \simeq 40$ s, the pressure response spectrum is almost densely populated, the system is in a strongly nonlinear regime. The figure 25 shows three representative spectra of each of these three phases. We can see the peaks in the first phase and the development of a "turbulent" spectrum in the last phase.
4. The forcing is globally constituted by a single line at the forcing frequency, which was expected. Nevertheless, from $t \simeq 38$ s, the spectrum of the forcing is populated with other frequencies. This is due to the fact that the gong system influences a bit the system that sets it in motion.

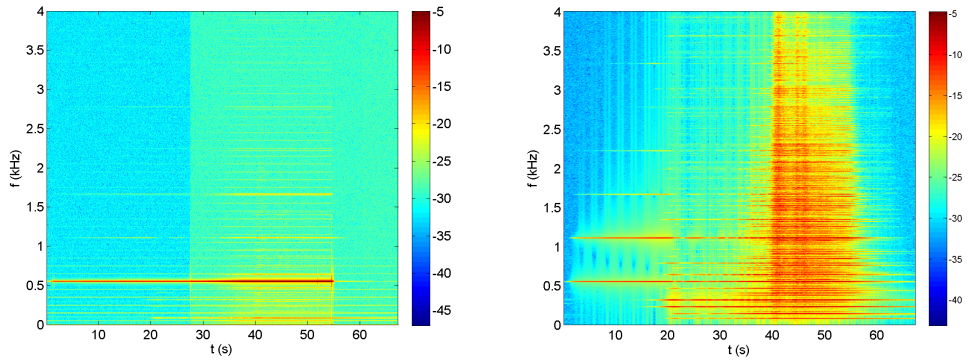

FIGURE 24 – Spectrograms of the forcing (left) and the gong pressure response signal (right) computed over 0.2 s time horizons at a frequency resolution $\Delta f = 5$ Hz.

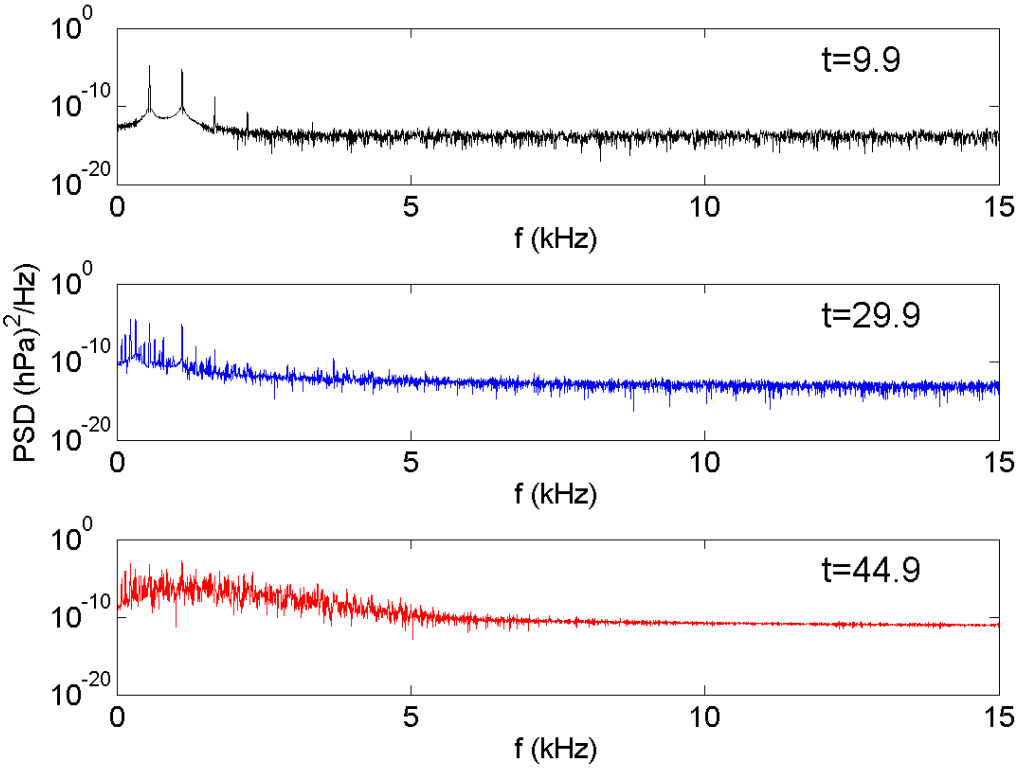

FIGURE 25 – Three spectra taken from the spectrogram of Fig. 24 at $t = 10$, 30 et 45 s (from top to bottom).